Diels-Alder reactions have shown the value of this approach.

An unsymmetrical cyclic TS for a pericyclic process in analogous to a cyclic conjugated hydrocarbon in which the CC bonds vary in length. Such a variation reduces[68] the aromatic or antiaromatic energy but it does not destroy it. There will therefore still be a tendency for two-bond pericyclic reactions to take place in a concerted manner, this tendency being stronger the less the resonance energies of the relevant bonds alternate in the cyclic TS. Reactions where the geometry of the cyclic TS disfavors the necessary overlap of orbitals will tend to take place in distinct one-bond steps and the tendency to retain stereochemistry will be correspondingly small; cf. the double electrocyclic ring opening of bicyclobutane (section C). These arguments emphasize the futility of attempts to discover synchronous pericyclic reactions in cases where the corresponding TS would be impossibly strained, on the grounds that they "ought" to occur because they are "allowed" by the Woodward-Hoffmann rules. The apparent power of the rule presented here also makes it seem extremely unlikely that *any* three-bond reaction can take place in a synchronous manner, for example, the trimerization of an olefin to a benzene derivative, unless four of the switching bonds are involved in migrations of hydrogen. The reduction of olefins by diimide would be an example of this and recent calculations by Olivella[69] indicate that it is indeed synchronous.

Summary and Conclusions

(1) The basic reactions of organic chemistry are mostly of one-bond type. Reasons are given for this, indicating that the activation energy of a synchronous two-bond reaction should be roughly double that of an analogous one-bond one. This conclusion is summarized in a new rule regulating the course of reactions; i.e., *synchronous multibond reactions are normally prohibited.* They occur only in specific cases where special circumstances make them unusually favorable.

(2) The only expected exceptions occur (a) when making/breaking bonds involve migration of a hydrogen atom from one atom to another, (X-H Y) → (X H-Y), particularly when one, or better still both, of the atoms X and Y are heteroatoms and (b) in cases where the activation energy of the synchronous reaction is very small, particularly when steric factors favor the synchronous mechanism in comparison with alternative two-stage or two-step ones.

(3) The only apparent exceptions to the new rule are the E2 reaction, the S_N2' reaction, and certain multibond pericyclic reactions that are "allowed" by the Woodward-Hoffmann rules.

(a) The E2 reaction has not been proved to be synchronous; however, it in any case exemplifies exception a above.

(b) Theoretical calculations indicate the S_N2' reaction to be a two-step process, formation of the new bond preceding rupture of the old one.

(c) Detailed analysis of the available data indicates that multibond pericyclic reactions, even if "allowed" by the Woodward-Hoffmann rules, nevertheless take place in a nonsynchronous manner if they violate the new rule and to not come under the heading of one of the expected exceptions to it.

(4) Many of the mechanisms suggested by the new rule have been supported by MINDO/3 and/or MNDO calculations, leading, in at least one case, to a mechanism that had not previously been considered and that yet is in agreement with all the available facts. In view of the success of these procedures in studies of a very large number of very varied reactions,[42,43] this both provides strong support for the new rule and also confirms the usefulness of MINDO/3 and MNDO as a guide to reaction mechanisms.

(5) Indications are given of possible applications of the new rule both in mechanistic studies and as an aid in organic synthesis.

Acknowledgment. This work was supported by the Air Force Office of Scientific Research (Contract AFOSR 79-0008) and the Robert A. Welch Foundation (Grant F-126).

(68) Dewar, M. J. S. *Tetrahedron, Suppl.* **1966**, *8*, 75.
(69) Personal communication from Dr. S. Olivella.

Cytochrome c_3 Modified Artificial Liposome. Structure, Electron Transport, and pH Gradient Generation

Iwao Tabushi,*† Takako Nishiya,*† Masatsugu Shimomura,‡,⊥ Toyoki Kunitake,‡,⊥ Hiroo Inokuchi,§,∞ and Tatsuhiko Yagi‖,∞

Contribution from the Department of Synthetic Chemistry, Kyoto University, Kyoto, 606 Japan, Department of Synthetic Chemistry, Kyushu University, Fukuoka, 812 Japan, Molecular Science Institute, Okazaki, 444 Japan, and Faculty of Education, Shizuoka University, Shizuoka, 422 Japan. *Received January 17, 1983*

Abstract: Detailed studies on the structure, electron transport rates, and proton transport rates coupled to electron transport were carried out for artificial lecithin liposomes functionalized with cyt c_3 or cyt *c*. Artificial liposomes modified with cyt c_3 were found to be single-walled, normal liposomes of ca. 250-Å diameter based on electron micrographs. The electron transport rate across the membrane was very much accelerated in the presence of cyt c_3, and the electron influx was coupled with rapid proton transport from the outside to the inside of the artificial liposome, generating a large pH gradient across the membrane. The maximum pH gradient is determined by the accelerated proton influx and slower passive proton efflux. The permeability coefficients of passive proton flow, P_{H^+}, and of accelerated coupled proton flow, P_{H^+}, were estimated. The observed permeability for the coupled transport is by a factor of 10^1-10^2 larger than the usual passive proton permeability.

In biological systems, the electrochemical potential gradient across the cell membrane is maintained by the inside-outside unequal distribution of lipids or proteins bound to the cell membrane. This potential difference induces the generation of a pH gradient or an ion concentration gradient across the membrane via coupling to a downhill chemical reaction. The pH gradient drives many important and complicated biological functions such as active transport,[1-4] stimulus-response,[5] and ATP synthesis.[6]

† Kyoto University.
‡ Kyushu University.
§ Molecular Science Institute.
‖ Shizuoka University.
⊥ Responsibile for a part of electron micrograph study.
∞ Responsible for a part of enzyme isolation study.

(1) Hokin, L. E., Ed. "Metabolic Pathways", 3rd ed.; Academic Press: New York, 1972; Vol. 6.
(2) Christensern, H. L. "Biological Transport", 2nd ed.; Benjamin: New York, 1975.
(3) Oxender, D. L. *Annu. Rev. Biochem.* **1972**, *41*, 777-809.

0002-7863/84/1506-0219$01.50/0 © 1984 American Chemical Society

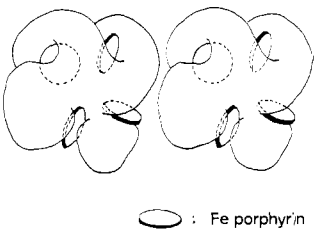

Figure 1. Schematic representation of heme orientation in cyt c_3.

Among these, the active transport of ions or other materials may be conveniently studied and understood in its foundamental aspects by using artificial membranes. One of the early examples of successful material transport across the liquid layer was reported by Lehn, who applied pH differences across a membrane.[7] This, together with many subsequent studies, revealed that material transport across an artificial membrane can be achieved by applying various types of chemical potential differences.

Electron transport across cell membranes plays a key role in ATP synthesis in mitochondria or chloroplasts. A better understanding of ATP synthesis caused by the electron transport across membranes may be obtained by the study of artificial systems displaying electron transport activity, which affords the necessary potential gradient for ATP synthesis. We have been able to prepare efficient electron transport systems for lecithin bimolecular membranes[8] or liquid membranes[9] functionalized with suitable electron carriers or an electron transport catalyst. Similarly, efficient electron transport has been shown for several other artificial electron transport systems by using bilayer lipid membranes[10-14] or liquid membranes[15-18] (Table I).

Recently, we prepared artificial liposomes functionalized with cyt c_3 from *Desulfovibrio vulgaris* MF (IAM 12604).[19] This enzyme is known to conduct electricity in the solid state, probably due to its strong intra- and interprotein heme–heme interaction (see Figure 1). It was observed that efficient electron transport from the external reductant, $Na_2S_2O_4$ or H_2/colloidal Pt, to an internal oxidant, $K_3Fe(CN)_6$, took place. Further, the formation of a pH gradient across the membrane associated with the electron transport was measured by the use of a newly prepared pH indicator, 2-chloro-1-naphthol-4,7-disulfonic acid.[20]

In this paper, we discuss a possible mechanism of pH gradient generation based on the following: (a) rapid H^+ transport associated with facilitated "downhill" electron flow, (b) preservation of electroneutrality, and (c) slower passive H^+ transport driven by the generated pH gradient across the membrane.

Table I. Artificial Electron Transport Systems[a]

electron donor	electron acceptor	mediator	ref
	Bilayer Membrane		
quinones	Fe^{3+}, Ce^{4+}	chloroplast	10
ASC	$K_3Fe(CN)_6$	ferrocene benzoquinone	11[b]
NaOCl	ASC	Hm-Mn(III)	8
ASC	$K_3Fe(CN)_6$	plastoquinone ubiquinone	12
EDTA	MV^{2+}	surfactant analogue of $Ru(bpy)_3^{2+}$	13
$Ru(bpy)_3^{2+}$	MV^{2+}		14
$Na_2S_2O_4$ colloidal Pt/H_2	$K_3Fe(CN)_6$	cyt c_3 C_4V^{2+}	19,42
	Liquid Membrane[c]		
MV^{2+}	indophenol methylene blue $FeCl_3$ cyt c	vitamin K_1 coenzyme Q	15
ASC $Na_2S_2O_4$ PF–MV^{2+}–EDTA	$K_3Fe(CN)_6$	vitamin K_3	16
ASC	$K_3Fe(CN)_6$	TMPD	17
$Na_2S_2O_4$ $(+K^+)$	$Na_3Fe(CN)_6$	Ni bisdithiolen–DC-18-C-6 complex (coupled transport of electron and metal)	18
$Na_2S_2O_3$ + $Zn^{2+}T_{SO_3Na}PP$	FMN	C_6V^{2+}	9

[a] ASC, ascorbic acid; MV^{2+}, methylviologen; $Ru(bpy)_3^{2+}$, tris(2,2′-bipyridine)Ru^{2+}; PF, proflavin; TMPD, *N,N,N′,N′*-tetramethyl-*p*-phenylenediamine; DC-18-C-6, dicyclohexyl-18-crown-6; Hm-Mn(III), hematoporphirin-Mn(III) complex; C_4V^{2+}, *N,N′*-di-*n*-butylviologen; C_6V^{2+}, *N,N′*-di-*n*-hexylviologen; $Zn^{2+}T_{SO_3Na}PP$; Zn^{2+} complex of sodium *meso*-tetraphenylporphyrintetra-*p*-sulfonate. [b] There is no description of actual experimental conditions; reported data are too qualitative to compare the electron transport rate with other studies. [c] Transport rates in liquid membrane systems are generally much smaller than that in bilayer membrane systems.

Experimental Section

Commercially available chemicals were used directly unless otherwise noted. Infrared spectra were obtained on a Hitachi Model 215 spectrophotometer. ^1H NMR spectra were recorded with Varian EM-360 and HA-100D instruments. Electronic spectra were measured with a Union SM-401 high-sensitivity spectrometer and a Hitachi 340S spectrophotometer. Fluorescence spectra were measured with a Union FS-301 high-sensitivity fluorescence spectrometer. pH measurement was performed on a Toa pH meter, Model HM 5-ES, instrument. Sonication was performed with a ultrasonic disruptor, Model UR-200P (Tomy Seiko). Centrifugation was carried out with a refrigerated centrifuge RS-20III (Tomy Seiko). For electron microscopy a Hitachi electron microscope, Model H-500, was used.

Materials. Egg lecithin was carefully purified according to the literature[21] and stored at −70 °C under Ar in the dark. Cyt c_3 was isolated from *D. vulgaris MF* (IAM 12604) and purified as described by Yagi.[22] Colloidal Pt supported on PVA (final concentration of Pt is 14 μequiv/L) was prepared according to the literature.[23] Freshly prepared colloidal Pt was used throughout the present experiments. *N,N′*-Di-*n*-butylviologen was prepared by usual method from γ,γ′-dipyridyl and *n*-butyl bromide by refluxing in CH_3CN.

Preparation of Artificial Liposome. Artificial liposomes incorporating $K_3Fe(CN)_6$ in their interior were prepared as follows. In 10 mL of $CHCl_3$ 80 mg of egg lecithin and 20 mg of bovine heart cardiolipin (Sigma) were dissolved, and then the solvent was gently removed under Ar in vacuo. The resulting lipid film was resuspended in 5 mL of a 0.5 M aqueous solution of $K_3Fe(CN)_6$ (5 mM Tris-HCl, pH 7.0), and the mixture was sonicated (5 min × 6, power 5) with external ice cooling in a box filled with Ar to avoid any air oxidation of lecithin.[24] To remove

(4) Kaczorowshi, G.; Shaw, L.; Fuentes, M.; Walsh, C. *J. Biol. Chem.* **1975**, *250*, 2855–2865.
(5) Metzler, D. E. "Biochemistry. The Chemical Reactions of Living Cells"; Academic Press: New York, 1977; pp 265–277.
(6) Henderson, P. J. *Annu. Rev. Microbiol.* **1971**, *25*, 393–428.
(7) Behr, J. P.; Lehn, J. M. *J. Am. Chem. Soc.* **1973**, *95*, 6108–6100.
(8) Tabushi, I.; Funakura, M. *J. Am. Chem. Soc.* **1976**, *98*, 4684–4685.
(9) Tabushi, I.; Yazaki, A.; Koga, N.; Iwasaki, K. *Tetrahedron Lett.* **1980**, *21*, 373–376.
(10) Tien, H. T. *Nature (London)* **1968**, *219*, 272–274.
(11) Hinkle, P. C. *Biochem. Biophys. Res. Commun.* **1970**, *41*, 1375–1381.
(12) Hauska, G. *FEBS Lett.* **1977**, *79*, 345–347.
(13) Ford, W. E.; Otvos, J. W.; Calvin, M. *Nature (London)* **1978**, *274*, 507–508.
(14) Tunuli, M. S.; Fendler, J. H. *J. Am. Chem. Soc.* **1981**, *103*, 2507–2513.
(15) Anderson, S. S.; Lyle, I. G.; Paterson, R. *Nature (London)* **1976**, *259*, 147–148.
(16) Grimaldi, J. J.; Boileau, S.; Lehn, J. M. *Nature (London)* **1977**, *265*, 229–230.
(17) Shinbo, T.; Kurihara, K.; Kobatake, Y.; Kano, N. *Nature (London)* **1977**, *270*, 277–278.
(18) Grimaldi, J. J.; Lehn, J. M. *J. Am. Chem. Soc.* **1979**, *101*, 1333–1334.
(19) Tabushi, I.; Nishiya, T.; Yagi, T.; Inokuchi, H. *J. Am. Chem. Soc.* **1981**, *103*, 6963–3965.
(20) Tabushi, I.; Nishiya, T. *Tetrahedron Lett.* **1982**, *23*, 2661–2665.
(21) Singleton, W. S.; Gray, M. S.; Srown, M. L.; White, J. L. *J. Am. Oil. Chem. Soc.* **1965**, *42*, 53–56.
(22) Yagi, T.; Maruyama, K. *Biochim. Biophys. Acta* **1971**, *243*, 214–224.
(23) Rampino, L. D.; Nord, F. F. *J. Am. Chem. Soc.* **1941**, *63*, 2745–2749.

small lecithin aggregate the solution was centrifugated at 20 000 rpm for 30 min and the supernatant was treated on a Sephadex 4B column (1.5 cm × 45 cm) at 4 °C with 5 mM aqueous Tris-HCl (pH 7.0) as the eluting buffer to separate bilayer liposome from unbound $K_3Fe(CN)_6$ and multibilayer liposomes. The artificial liposomes (abbreviated as Fe^{III}-(i)|Lip^- hereafter) contain $K_3Fe(CN)_6$ in their interior and carry negative charges of cardiolipin on the membrane. They eluted from the column within 2 h and had an absorption at 420 nm characteristic of $K_3Fe(CN)_6$ and at 215 nm characteristic of artificial liposome.

Artificial liposomes containing $K_3Fe(CN)_6$ and 2-chloro-1-naphthol-4,7-disulfonic acid as a pH indicator (Fe^{III}(i)·CNDS(i)|Lip^-; the indicator was abbreviated as CNDS hereafter) were prepared by the same method as described above except that the lipid film was resuspended in 5 mL of a buffer solution (1 mM Tris-HCl, pH 7.0) containing $K_3Fe(CN)_6$ (0.17 M) and an appropriate amount of the disulfonic acid. Artificial liposomes containing only CNDS in its interior [CNDS(i)|Lip^-] were also prepared by the same method as described above except that the lipid film was resuspended in 5 mL of a buffer solution (1 mM Tris-HCl, pH 7.0) containing an appropriate amount of the disulfonic acid.

Functionalization of Artificial Liposomes. Treatment of artificial liposomes, Fe^{III}(i)|Lip^- (a), Fe^{III}(i)·CNDS(i)|Lip^- (b), and CNDS(i)|Lip^- (c), with cyt c_3, cyt c, and C_4V^{2+} (abbreviation of *N,N'*-di-*n*-butylviologen) gave the following "functionalized" artificial liposomes: Fe^{III}(i)|-Lip^-·cyt c_3 (**1**); Fe^{III}(i)|Lip^-·(C_4V^{2+})·cyt c_3 (**2**); Fe^{III}(i)|Lip^-·C_4V^{2+} (**3**); Fe^{III}(i)|Lip^-·cyt c (**4**); Fe^{III}(i)·CNDS(i)|Lip^-·cyt c_3 (**5**); Fe^{III}(i)·CNDS-(i)|Lip^-·C_4V^{2+} (**6**); CNDS(i)|Lip^-·cyt c_3 (**7**); CNDS(i)|Lip^-·C_4V^{2+} (**8**). A general method of the functionalization is as follows. To the freshly prepared artificial liposome solution (1.0 mL) described previously, a, b, or c, an appropriate amount (0.05–0.33 mL) of a 120 μm aqueous solution of cyt c_3 and/or 400 μM aqueous solution of C_4V^{2+} or an appropriate amount (0.05–0.28 mL) of a 120 μM aqueous solution of cyt c (from horse heart, Sigma type III) was added dropwise with gentle stirring for 1 min at room temperature. Then the volume of the solution was adjusted to 2.0 mL by the addition of the buffer solution (5 mM Tris-HCl, pH 7.0, for **1–4**; 1 mM Tris-HCl, pH 7.0, for **5–8**. The functionalized liposomes, **1–8**, were separated and purified through a Sephadex G-50 column (0.7 cm × 30 cm) at 4 °C within 30 min. The eluting buffer was 5 mM Tris-HCl, pH 7.0, for **1–4** and 1 mM Tris-HCl, pH 7.0, for **5–8**.

The apparent (analytical) concentrations of cyt c_3 and cyt c were estimated from the characteristic absorption at 552 nm ($\epsilon = 1.10 \times 10^5$) and 550 nm ($\epsilon = 2.77 \times 10^4$), respectively, after complete reduction of the enzyme by addition of a small amount of solid $Na_2S_2O_4$. The bulk (analytical) concentration of internal $K_3Fe(CN)_6$ was determined by electronic spectra at λ_{max} 435 nm ($\epsilon = 880$). Oxidized forms of cyt c_3 and cyt c have large absorption at 435 nm, with $\epsilon = 8.45 \times 10^4$ and $\epsilon = 2.15 \times 10^4$, respectively. Therefore, for the liposomes containing cyt c_3 or cyt c the absorbance of $K_3Fe(CN)_6$ at 435 nm was calculated by subtracting the absorbance of the oxidized form of cyt c_3 or cyt c (concentrations of the enzymes were determined as described above) from the observed absorbance. From the absorbance the concentration of the internal $K_3Fe(CN)_6$ was estimated to be 110 mM for functionalized liposomes **1–4** and 37 mM for **5** and **6** by making a necessary correction for the internal/external volume ratio. The spectrum of the same concentration of the liposome solution containing neither $K_3Fe(CN)_6$ nor an electron carrier was used as a standard. The bulk (analytical) concentration of internal CNDS was determined from the comparison between the acid-treated liposome and the alkali-treated liposome (vide infra) by observing the characteristic absorption of dissociated form of CNDS at 360 nm.

Penetration of Cyt c_3 into Membrane. To examine the effect of "after-sonication" on penetration of cyt c_3 into the membrane, the artificial liposome Fe^{III}(i)|Lip^-·cyt c_3 freshly prepared as described above was further sonicated. Thus, after the addition of cyt c_3 to the solution of freshly prepared Fe^{III}(i)|Lip^-, the combined solution was briefly sonicated for 6 min[25] and the resultant liposome was separated through a Sephadex G-50 column by the same method as described above. The resultant cyt c_3 liposome, after application of after-sonication, was eluted from a Sephadex G-50 column at the same retention volume as the original liposome and its electronic spectrum was practically identical with that of the original liposome.

Reduction of the Functionalized Liposome with $Na_2S_2O_4$. A solution of the artificial liposome **1** or **4** (1.95 mL) was placed in a cell equipped with a three-way stopcock and the solution was deaerated through careful substitution of air by Ar via repeated evacuation and Ar introduction. The deaerated solution was mixed with a 0.05 mL of freshly prepared aqueous $Na_2S_2O_4$ solution by the use of a specially designed syringe that has small holes and a closed tip as reported in the previous paper.[19] An aqueous $Na_2S_2O_4$ solution was prepared by dissolving 60 mg of fresh $Na_2S_2O_4$ in 10 mL of 5 mM Tris-HCl buffer (pH became 7.0), and the final concentration of $Na_2S_2O_4$ after mixing with the liposome solution was determined by $K_3Fe(CN)_6$ titration[26] to be 670 μM. The reduction of internal $K_3Fe(CN)_6$ was followed by the intensity change of its visible absorption at 435 nm. The absorption of cyt c_3 or cyt c was ascertained not to interfere seriously with the above measurement because of the following facts: (a) the contribution of the cyt absorption change to the total absorption change was less than 23% under the conditions, (b) the change in the $K_3Fe(CN)_6$ concentration was measured where the oxidized and the reduced form of the cyt was practically in the steady state. The reduction of cyt c_3 or cyt c was followed by the intensity change of the characteristic absorptions of the reduced forms, at 552 and 550 nm, respectively. All the measurements were carried out in 5 mM aqueous Tris-HCl buffer solution at pH 7.0, 27 °C.

Hydrogen "Metabolism" Experiments by the Functionalized Liposomes. Measurements of hydrogen "metabolism" by the artificial liposomes were carried out as follows. By the use of an apparatus described above, vigorous H_2 bubbling was applied for 5 min to 1.95 mL of the aqueous solution of the functionalized liposomes **1–6**. The resultant solution was mixed with 0.05 mL of an aqueous solution of colloidal Pt supported on PVA (final concentration of K_2PtCl_4 was 14 μM) by use of a specially designed syringe. The reaction was followed by measuring the electronic spectrum change at 435 nm for the $K_3Fe(CN)_6$ decrease as described above. The dissociated form of CNDS showed characteristic absorptions at 360 and 340 nm. The former has the larger absorbance change between dissociated and undissociated forms but the spectral change at 340 nm was less affected by the interfering spectral change of c_3 or $K_3Fe(CN)_6$ (less than 15%, combined). The reduction of cyt c_3 and cyt c was followed by measuring the absorptions at 552 and 550 nm, respectively. Measurements for **1–4** were carried out in a 5 mM Tris-HCl buffer at pH 7.0 at 27 °C and measurements for **5** and **6** were carried out in a 1 mM Tris-HCl buffer at pH 7.0 at 27 °C.

Stability of Artificial Liposome. After the electron transport experiments were over, sample solutions were combined for each kind of functionalized artificial liposome, **1–6**, and 8 mL of the combined solution was concentrated to 2 mL by the use of ultrafiltration membrane cones (Centriflow CF 50A, Amicon). The resultant condensed solution was analyzed by gel filtration on a Sephadex G-50 column and also by electronic spectroscopy. Each of the recovered artificial liposome was eluted from the column at the same retention volume as the corresponding functionalized liposome before the electron transport experiments. In the recovered liposome 98.5–99.5% of $K_3Fe(CN)_6$ (probably due to air reoxidation) and 95.3–96.7% of CNDS remained unchanged after 36 h from separation of artificial liposomes 1–6, as determined by the electronic absorption at 420 and 360 nm, respectively. Corresponding amounts of free CNDS and $K_3Fe(CN)_6$ were recovered from eluents of larger retention volumes. Similar experiments were performed on artificial liposomes Fe^{III}(i)|Lip^- and CNDS(i)|Lip^- before the electron transport experiments and the amounts of $K_3Fe(CN)_6$ and CNDS eluting out of the liposomes were determined for several samples after 70–144 h. From these results, ca. 1% of $K_3Fe(CN)_6$ and 4% of CNDS originally present in the interior of the artificial liposome were shown to elute out after 36 h from the separation. Since kinetic measurements take 20–30 min, leakage of $K_3Fe(CN)_6$ or CNDS during the kinetic studies is negligible. Therefore, it is concluded that the original shape, size, and composition of the artificial liposome modified with enzyme or C_4V^{2+} were preserved after the electron transport experiments and permeabilities of artificial liposome membrane, **1–6**, to $K_3Fe(CN)_6$ and CNDS were not affected by modification with cyt c_3 or C_4V^{2+}.

Determination of Phospholipid Concentration. The phospholipid concentration of the liposome solution used for electron transport and/or proton transport was determined to be 5.55×10^{-3} M by the method of Bartlett.[27]

Electron Microscopy. A solution (1.0 mL) of Fe^{III}(i)|Lip^- (1.4 μM) was mixed with 1 mL of 2% aqueous phosphotungstic acid (pH 7.0) and sonicated for 15 min under N_2 atmosphere. The mixture was incubated in ice–water for 30 min and allowed to stand at room temperature for 1 h. After addition of cyt c_3, a small amount of the mixture was applied to the carbon-coated Cu mesh, dried, and subjected to electron microscopic examination.

Measurements of Internal pH and the Amount of Transported H^+ and/or OH^- Coupled to Electron Transport. Two kinds of liposome solutions were prepared, the external pH being adjusted to 4.0 and 11.0,

(24) Autoxidation of lecithin is relatively rapid. Examination of liposome preparations is necessary during the experimental procedures, which can be done by measurement of the change in absorption at 233 nm.

(25) Racker, E. *Biochim. Biophys. Res. Commun.* **1973**, *55*, 224–230.

(26) Creutz, C.; Sutin, N. *Proc. Natl. Acad. Sci. U.S.A.* **1973**, *70*, 1701–1703.

(27) Bartlett, G. R. *J. Biol. Chem.* **1959**, *234*, 466–468.

Figure 2. Electron micrograph of artificial liposome modified with cyt c_3. Magnification 60 000×.

for every artificial liposome **5–8**. The liposome solution was allowed to stand overnight at 4 °C to make the internal pH equal to the external pH. The internal pH was determined experimentally from the calibration line for the ratio of the concentration of the dissociated form of CNDS to that of free form (I^-/IH) vs. pH value independently measured under similar conditions. The internal pH of the liposomes **5–8** was affected by Tris-HCl and CNDS itself. Therefore, the amount of H^+ and/or OH^- transported across the membrane was estimated by using another calibration curve for the pH change vs. HCl added under the electron transport conditions.

Thus, 100 mL of a CNDS aqueous solution of 1 mM Tris-HCl buffer (3.4×10^{-4}–3.4×10^{-3} M) was titrated with HCl (0.02–0.2 N) starting at pH 7.0, and the I^-/IH value was obtained from the spectral change at 340 nm during the HCl titration.

Passive Transport of H^+. Passive transport rates of H^+ were measured for the following functionalized artificial liposomes—CNDS(i)|Lip^-, CNDS(i)|Lip^-·cyt c_3, and CNDS(i)|Lip^-·C_4V^{2+}—by applying the appropriate pH gradient across the membrane. A solution of CNDS(i)|Lip^- in 1 mM Tris-HCl buffered at pH 7.0 (1.75 mL) and 0.05 mL of a $^1/_{30}$ N aqueous HCl solution were rapidly mixed by the use of a specially designed syringe,[19] and the spectral change at 340 nm vs. time was measured to estimate the internal pH value. The external pH value after mixing was 3.8. Similar experiment was performed by using 0.05 mL of $^1/_{50}$ N HCl, where the external final pH was 4.5. Passive transport rates of H^+ for liposomes **7** (average concentration of cyt c_3 being 5.4 μM) and **8** (average concentration of C_4V^{2+} being 10 μM) in 1 mM Tris-HCl buffer were also measured at pH 7.0 as described above except that 0.05 mL of $^1/_{100}$ N HCl was used for **7**. Under the conditions the final external pH was 6.1, which is appropriate to avoid any denaturation of cyt c_3 in acidic solution.

Results and Discussion

Structure of Artificial Liposomes. As shown in Figure 2 electron micrographs of artificial liposomes modified with cyt c_3 [Fe^{III}(i)|Lip^-·cyt c_3] clearly demonstrate a closed, single-compartment bimolecular liposomal structure with diameters of ca. 250 Å and membrane width of ca. 40 Å. On the basis of the electron micrograph the following estimates for Fe^{III}(i)|Lip^-·cyt c_3 were made: molecular weight, 4.91×10^6 (including interior water and assuming that specific gravity of a lipsome as a whole is unity); aggregation number of phospholipid, 4.0×10^3;[28] volume of the interior solution of a single liposome, 2.57×10^{-18} cm^3. These values are in excellent agreement with those estimated by Huang:[29] specific gravity of liposome, 1.012; molecular weight, 2.06×10^6 (not including interior water); aggregation number, 2678. Thus, the electron micrograph results indicate that the present artificial liposomes modified with cyt c_3 [Fe^{III}(i)|Lip^-·cyt c_3] keep the ordinary bimolecular liposomal structure with normal size and shape, in accordance with the observed gel permeation behavior. Other modified artificial liposomes showed very similar gel permeation behavior and spectroscopic characteristics, demonstrating that their liposomal structures were the same as unmodified or cyt c_3 modified artificial liposomes. The phospholipid concentration of the presently used liposome solution was directly determined to be 5.55×10^{-3} M for the most frequently studied liposome concentration. By use of this value, and the aggregation number estimated above, the concentration of liposomes was calculated to be about 1.4×10^{-6} M. On the basis of this value, a ratio of the external volume of the bulk aqueous solution to the combined internal volume of the liposome is around 460. For every functionalized liposome, leakage of a variety of ions or hydrophilic compounds from the interior (passive transport across the membrane) was shown to be very slow.

Table II. Reduction Rate Constant of $K_3Fe(CN)_6$ in the Cyt c_3 Functionalized Liposomes[d]

N_{c_3}[c]	conen of $Na_2S_2O_4$, mM	bulk conen of $K_3Fe(CN)_6$, mM	k, s^{-1}	$k/N_{c_3}^2 \times 10^3$
2.55[b]	0.94	0.24	0.029	
2.55[b]	1.62	0.24	0.038	
2.55[b]	2.79	0.24	0.048	
2.55[b]	0.94	0.12	0.026	
7.71[a]	0.67	0.24	0.230	3.87
6.21[b]	0.67	0.24	0.149	3.86
4.64[b]	0.67	0.24	0.080	3.72
4.19[b]	0.67	0.24	0.065	3.70
3.86[a]	0.67	0.24	0.055	3.69
3.57[b]	0.67	0.24	0.047	3.69
3.21[b]	0.67	0.24	0.038	3.69
2.92[b]	0.67	0.24	0.031	3.64
2.55[b]	0.67	0.24	0.023	3.54
2.14[b]	0.67	0.24	0.016	3.49
1.14[b]	0.67	0.24	0.0028	

membrane modification (no. of molecules/liposome)	k, s^{-1}
H_2/Colloidal Pt Reduction	
without modification	~0
cyt c_3 (4.64)	0.0020
cyt c_3 (4.64) + C_4V^{2+} (7.14)	0.065
C_4V^{2+} (7.14)	0.0015
	0.0014[e]
C_8V^{2+} (7.14)	8.6×10^{-5}
cyt c (4.64)	(0.03×10^{-3})

[a] With further sonication (see the text). [b] Without further sonication. [c] Average number of cyt c_3 on a single liposome particle. [d] $k_0 = 0.0010$ s^{-1} (without cyt c_3. [e] Reaction was started at inside pH 6.0 and outside pH 7.0.

Thus, the concentration of the internal CNDS was calculated by eq 1, where subscripts i and anal. mean interior concentration and average "analytical" concentration of the solution as a whole. Concentrations of other species present in the interior aqueous solution were similarly calculated based on the analytical values.

$$[CNDS]_i = 460[CNDS]_{anal.} \quad (1)$$

Electron Transport in Artificial Liposomes Modified with Cyt c_3. The solution of the liposome modified with cyt c_3 [Fe^{III}(i)|Lip^-·cyt c_3] was reduced with external aqueous $Na_2S_2O_4$, and the decrease of the interior Fe^{III} concentration was followed by the change of absorbance at 435 nm. As described in previous papers, rapid conversion of cyt c_3^{III} to cyt c_3^{II} and a slower pseudo-first-order decrease of ferricyanide were observed[19] (k_1, eq 2). Careful investigation of the rate equation for different initial concentrations of components indicates that the rate is of $^1/_2$ order with respect to $Na_2S_2O_4$. The results are summarized in Table II and Figure 3. Two striking characteristics of Fe^{III}(i)|Lip^-·cyt c_3 were observed: (i) very efficient electron transport across the membrane (facilitated electron transport), much more efficient than that of the cyt c membrane, which is known as a typical electron transporting system (see Table III);

$$-\frac{d[Fe(CN)_6^{3-}]}{dt} = k_1[Fe(CN)_6^{3-}] \quad (2)$$

$$-\frac{d[Fe(CN)_6^{3-}]}{dt} = k[Fe(CN)_6^{3-}][S_2O_4^{2-}]^{1/2} \quad (3)$$

(28) The aggregation number was estimated from the calculated weight of membrane divided by molecular weight of phospholipid. The weight of membrane, 3.37×10^6, was calculated from the average molecular weight (849) and the volume of membrane that was calculated by taking the specific gravity of liposome as unity. The statistically average molecular weight was calculated based on the fact that the liposome was prepared from 1.03×10^{-4} mol of lecithin (M_r 775) and 0.14×10^{-4} mol of cardiolipin (M_r 1394).

(29) Huang, C. *Biochemistry* **1969**, *8*, 344–352.

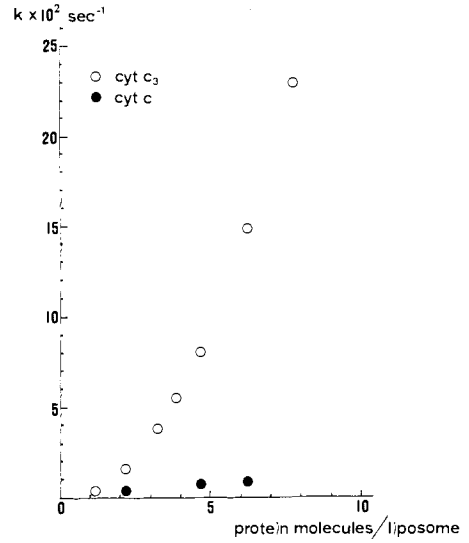

Figure 3. Dependence of k on the concentration of enzyme.

(ii) a significant contribution of second-order kinetics with respect to cyt c_3 (eq 4), the term being responsible for efficient electron transport (see Table II and Figure 3):

$$k_1 = k_3[c_3]^2 + k_2[c_3] \qquad k_3 \gg k_2 \tag{4}$$
$$k_1 = k_{app} - k_0$$

where k_{app} is the apparent first-order rate constant for the ferricyanide reduction in the cyt c_3 liposome interior and k_0 is the apparent first-order rate constant for the ferricyanide reduction in the liposome interior without cyt c_3 modification.

The second characteristic is noteworthy. The average distance, d_{av}, between cyt c_3 molecules on the membrane was estimated to be at least ca. 160 Å[30] by using eq 5[19] for the lipsome modified with an average of 7.7 cyt c_3 molecules (highest concentration) per single liposomal particle.

$$d_{av} = \left(\frac{4\pi r^2}{N}\right)^{1/2} \qquad N = \frac{\text{concn of cyt } c_3}{\text{concn of liposome}} \tag{5}$$

Therefore, the observed second-order kinetics, with respect to cyt c_3, strongly suggest that two cyt c_3 molecules associate for at least a short period and, through this aggregate, electrons are transported much more efficiently than through isolated cyt c_3.

Formation of Cyt c_3 Dimer as an Electron Channel. Under the present conditions, lateral diffusion of cyt c_3 through the lecithin liposomal membrane described by eq 6[31] is quite rapid, being

$$D_T = kT/(6\pi\eta a) \tag{6}$$

calculated to be 2.9×10^{-9} cm²/s. On the basis of the assumption that an enzyme molecule occupies either an exterior or interior site due to its hydrophilicity and that the size of the site is equal to the cross section of the enzyme, a probability of dimer formation, P_T, can be calculated by use of D_T.

$$P_T = {}_lC_2 \cdot \frac{D_T}{d_E}\frac{S_E}{s_L} \cdot p = {}_lC_2 \cdot 207 \cdot p \text{ s}^{-1} \tag{7}$$

In eq 7, S_E and d_E are the cross section and diameter of the enzyme, respectively. p is the probability of the site contact ($1 \geq p \geq 9$).[32] l is a number of enzyme molecules in a single liposome particle. Therefore, it is concluded that the probability of channel formation is great enough for effective electron transport.[32]

This electron channel mechanism is in good agreement with the observed high electric conductance of the solid cyt c_3 layer, indicating that the intermolecular (interprotein) electron transfer between two (or more) cyt c_3 molecules is extremely efficient. To confirm satisfactory penetration of cyt c_3 molecules into the membrane, the electron transport rate, which was second order with respect to cyt c_3, was measured for two types of the artificial liposome, $Fe^{III}(i)|Lip^-\cdot$cyt c_3 with and without prolonged sonication (see Table II). The second-order rate constants were practically the same. Therefore, we conclude that cyt c_3 molecules in the presence of cardiolipin penetrate satisfactorily into the liposomal membrane, even without further prolonged sonication.

The present mechanism of cyt c_3 aggregation is consistent with the X-ray crystallographic results that a cyt c_3 molecule has an approximately spherical shape of ca. 30-Å diameter,[33] while the thickness of the liposomal membrane is 40–50 Å.[34-37] The relative inefficiency of electron transport through isolated cyt c_3 molecules is compatible with the very slow electron transport through the corresponding cyt c membrane, $Fe^{III}(i)|Lip^-\cdot$cyt c, where electrons were transported only via a first-order kinetic process with respect to cyt c (see Figure 3), indicating the significance of the "carrier" mechanism. Therefore, we conclude that "electron channel" formation by the self-aggregation of cyt c_3 on the artificial membrane is a unique and an interesting characteristic of cyt c_3.

Hydrogen-"Metabolizing" Liposomes. In sulfate-reducing bacteria, hydrogenase and cyt c_3 catalyze the metabolism of H_2 or other organic or inorganic reducing reagents for the purpose of the ATP synthesis using sulfate as an oxidizing reagent. The hydrogenase has two cubic iron–sulfur complexes in its active site to facilitate the electron transfer from H_2 to cyt c_3 (eq 8). The

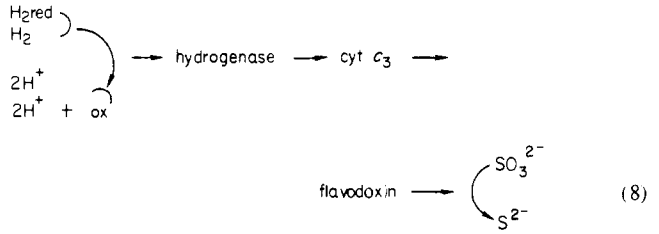

(8)

major chemical function of the hydrogenase seems to be to reduce the potential barrier for the conversion of H_2 into H^+ by weakening the H–H bond through absorption of H_2 on the iron–sulfur complex and/or polarization, probably by hydrogen bonding.[38]

However, the detailed structure of the hydrogenase has not yet been clarified. To gain further insight into the mechanism of this interesting catalysis, the possible activation of H_2 must be investigated in more detail. However, the reduction potential of most artificial cubic iron–sulfur complexes are too high (−1.91 ~ −0.6 V NHE) to activate H_2 $E_0 = -0.42$ V) effectively. We have been studying the catalytic activity of colloidal Pt supported on polyvinylpyrrolidone (PVP) or polyvinyl alcohol (PVA) for activation of H_2.[39] In the electron transporting liposomes studied here, colloidal Pt on PVA was used to activate H_2, an appropriate electron source. The solution of liposomes modified with cyt c_3, $Fe^{III}(i)|Lip^-\cdot$cyt c_3 (bulk concentration = 6.5 μM corresponding to 4.6 cyt c_3 molecules per single liposomal particle), was reduced by bubbling H_2 in the presence of colloidal Pt. The decrease of interior Fe^{III} concentration was followed by observing the change of absorbance at 435 nm. Again rapid conversion of cyt c_3^{III} to cyt c_3^{II} was observed, reaching a stationary state within 1 s where a ratio, c_3^{II}/c_3^{III}, was constant. This very rapid reaction was followed by the slower pseudo-first-order decrease of $K_3Fe(CN)_6$. Results are summarized in Table III. As

(30) ca. 240 Å for 3.4 cyt c_3 molecules per single liposomal particle.
(31) Saffman, P. G.; Delbruck, M. *Proc. Natl. Acad. Sci. U.S.A.* **1975**, *72*, 311–3113.
(32) A detailed discussion will be made in a forthcomming article.
(33) Higuchi, Y.; Yasuoka, N.; Kakudo, M.; Yagi, T.; Inokuchi, H. *J. Biochem. (Tokyo)* **1981**, *89*, 1659–1662.
(34) Brown, L. R.; Wuthrich, K. *Biochim. Biophys. Acta* **1977**, *468*, 389–410.
(35) Gulik-Kryzwicki, T.; Shechter, E.; Luzzati, V.; Faure, M. *Nature (London)* **1969**, *223*, 1116–1121.
(36) Shipley, G. G.; Leslie, R. B.; Chapman, D. *Nature (London)* **1969**, *222*, 561–562.
(37) Blaurock, A. *Biophys. J.* **1973**, *13*, 290–298.
(38) Yagi, T.; Tsuda, M.; Inokuchi, H. *J. Biochem. (Tokyo)* **1973**, *73*, 1069–1081.
(39) Tabushi, I.; Yazaki, A. *J. Am. Chem. Soc.* **1981**, *103*, 7371–7373.

Table III. Membrane Functionalization and Electron Transport Rate: $Na_2S_2O_4$ Reduction

membrane modification (no. of molecules/liposome)	k, s^{-1}
cyt c_3 (1.14–7.71)	(see Table II)
cyt c_3 (4.19) + C_4V^{2+} (7.14)	0.061
cyt c_3 (3.57) + C_4V^{2+} (7.14)	0.047
cyt c_3 (2.92) + C_4V^{2+} (7.14)	0.031
C_4V^{2+} (7.14)	0.0023
cyt c (6.21)	0.0075
cyt c (4.64)	0.0070
cyt c (2.14)	0.0030

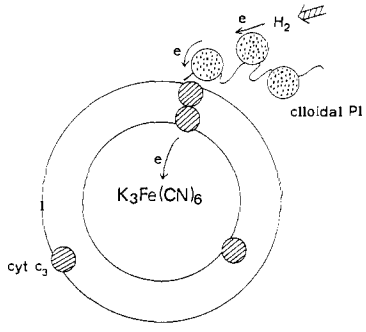

Figure 4. Schematic representation of electron channel in cyt c_3 functionalized liposome.

shown in Table III, colloidal Pt is a very efficient catalyst for electron transport from external H_2 to internal $Fe(CN)_6^{3-}$ via the cyt c_3 membrane, while for the liposome modified with cyt c [Fe^{III}(i)|Lip^-·cyt c] the observed initial reduction rate of cyt c^{III} was considerably slower ($\tau_{1/2}$ = 20 s) and the reduction of $K_3Fe(CN)_6$ across the cyt c membrane was much slower. The oxidation–reduction potential of cyt c is +0.25 V (NHE), being considerably more positive than those of cyt c_3: −0.34, −0.30, −0.28, and −0.23 V (NHE). Considering these potentials, the observed much faster electron transport from external H_2 to internal aqueous $K_3Fe(CN)_6$ across the liposomal membrane modified with cyt c than the cyt c_3 liposome may be expected. However, the observed cyt c reduction rate was much slower than that for cyt c_3, when the enzymes were bound to the artificial liposomal membrane. Again, this strongly supports the present mechanism: (a) the "jutting" orientation of aggregating cyt c_3 molecules from the external membrane surface into the interior aqueous solution (see Figure 4) and (b) rapid electron transfer between cyt c_3 molecules—if not, about half of the cyt c_3 molecules should be reduced relatively slowly.

Generation of a pH Gradient across the Membrane, Coupled to Electron Transport. Rapid transport of electrons into the artificial liposomes from the exterior bulk solution would violate the electroneutrality condition of the internal solution, if electron transport alone took place without cotransport of a cation and/or counter transport of an anion. Under our experimental conditions, cotransport of H^+ and/or counter transport of OH^- must be important because of the extreme permeability of phospholipid membrane to H^+ and OH^- (see Table IV). The transport of H^+ and/or OH^- (hereafter two types of transport will be combined and described as "H^+" transport for simplicity) necessarily generates a pH gradient across the membrane if all of the passive transport processes take place much more slowly than coupled transport. To estimate the pH gradient generated, fluorescence measurements (e.g., 9-aminoacridine) are usually used.[40] However, this method cannot be used for the present liposome systems because of the serious quenching of 9-aminoacridine fluorescence by Fe^{III} [quenching constant was estimated to be 1.7×10^3 M^{-1} from the Stern–Volmer plot; however, the plot deviates from a straight line in the presence of a high concentration of $K_3Fe(CN)_6$]. H^+ transport coupled to electron transport can also be monitored by an appropriate pH indicator incorporated into the interior of the artificial liposome. To be used in our system, an indicator must fulfill the following requirements: (i) it should not be reducible under a strongly reducing conditions (cyt c_3^{II} or C_4V^+), (ii) it should have pK_a value near 7 in order to be sensitive to the pH change around 7, (iii) it should be strongly hydrophilic to avoid appreciable binding to the membrane core, and (iv) its molar absorption coefficient should be large. Most of the indicators available are readily reduced with $Na_2S_2O_4$ or H_2/colloidal Pt and/or oxidized with $K_3Fe(CN)_6$ and are not appropriate for the present purposes. A relatively satisfactory indicator, disodium 2-naphthol-3,6-disulfonate, **1**, was first used as the pH indicator.

Table IV. Permeability of Ions Abundant in Living Systems[b]

ion	P, cm/s large liposome	P, cm/s small liposome
H^+ and OH^-	1.4×10^{-4} [41] (PC/PA 98/2)	1.1×10^{-8} [a] (PC/CL 88/12)
Na^+	1.0×10^{-10} [41] (PC/PA 98/2)	1.1×10^{-13} [47] (PC/PA 96/4); 1.2×10^{-14} [48] (PC)
Cl^-	$\sim 10^{-8}$ (PC/PA 98/2)	6.5×10^{-12} [47] (PS); 3.7×10^{-12} [47] (PS/Chol 50/50)

[a] Present results. [b] PC, phosphatidylcholine; PA, phosphatidic acid; CL, cardiolipin; PS, phosphatidylserine; Chol, cholesterol. Numbers in parentheses show mol % of phospholipid.

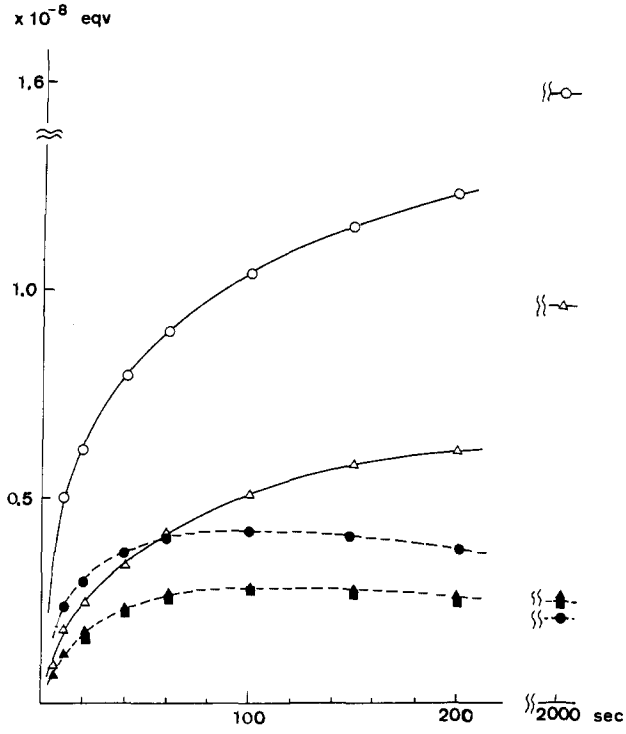

Figure 5. Transport of H^+ coupled with electron transport. cyt c_3–liposome: (○) Total amount of electrons transported; (●) total amount of H^+ transported, [CNDS] = 1.64×10^{-3} M. C_4V^{2+}–liposome: (△) electron; (▲) H^+, [CNDS] = 0.34×10^{-3} M; (■) H^+, [CNDS] = 2.04×10^{-3} M.

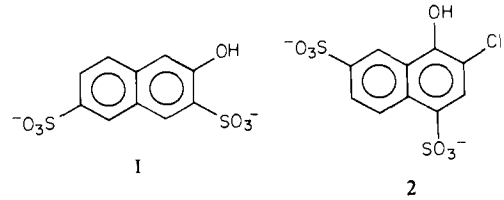

1 2

(40) Nichols, J. W.; Hill, M. W.; Bangham, A. D.; Deamer, D. W. *Biochim. Biophys. Acta* **1980**, *596*, 393–403.

Table V. Maximum pH Gradient Generated across the Membrane

	C_4V^{2+}–liposome		c_3–liposome
concn of CNDS	2.04×10^{-3}	0.34×10^{-3}	1.64×10^{-3}
$\Delta[H^+]_{influx}$, equiv	0.26×10^{-8}	0.27×10^{-8}	0.42×10^{-8}
obsd pH(i)	6.5	5.95	6.25
pH(i) without buffer and CNDS	3.21		3.01

The pH gradient thus observed was 0.01,[41] when the electron transport was started from pH 9.0 (pK_a of the indicator = 9.5). As an satisfactory indicator having a pK_a value near 7, CNDS, **2**, was prepared and the pK_a value of this new indicator was determined as 6.2 by the electronic spectrum–pH titration. In the reduction of Fe^{III}(i)·CNDS(i)|Lip^-·C_4V^{2+} or Fe^{III}(i)·CNDS(i)|Lip^-·cyt c_3 with H_2/colloidal Pt(0) at pH 7.0, the amount of H^+ transported was approximately equal to that of transported electrons in the early stages of the reaction (Figure 5). Then the H^+ gradient gradually decreased after passing through a broad maximum. The observed maximal pH gradients generated across the membrane are shown in Table V. In the presence of the indicator and the Tris buffer, a major amount of the protons flowing into the liposome interior was consumed by neutralization of the indicator anion and the buffer. Thus, the observed maximal pH gradient reached 0.5 and 1.05 after 100 s when the concentration was 2.04×10^{-3} and 0.34×10^{-3} M, respectively. In a series of these experiments, the total amount of $\Delta[H^+]_{o\to i} + \Delta[OH^-]_{i\to o}$ (hereafter abbreviated as $\Delta = \Delta[H^+]_{o\to i} + \Delta[OH^-]_{i\to o}$) was found to be practically constant, independent of the buffer and indicator concentrations.

Therefore, it is quite safe and reasonable to extrapolate the observed pH gradient for a series of indicator and Tris buffer concentrations to the zero concentration of indicator and buffer (Table V). The extrapolation gives a maximum pH gradient Δ_{max} of 3.8 and 4.0 for the C_4V^{2+} liposome and the cyt c_3 liposome, respectively (Table V). The magnitude of this pH gradient is large enough for effective ATP synthesis. Therefore, if the ATP synthesis system is further attached to the liposome, a complete H_2-metabolizing artificial cell able to synthesize ATP may be available (see Table V).

Maximum pH Gradient and Passive Proton Leakage. The gradual decrease of the pH gradient after the broad maximum observed for the reduction of Fe^{III}(i)·CNDS(i)|Lip^-·C_4V^{2+} or Fe^{III}(i)·CNDS(i)|Lip^-·cyt c_3 with H_2/colloidal Pt supported on PVA seems to be due to the passive transport of H^+ driven by the pH gradient temporarily generated across the membrane by coupling to the rapid electron flow. The passive H^+ transport rates across the lecithin bilayer membrane of the functionalized artificial liposomes CNDS(i)|Lip^-, CNDS(i)|Lip^-·cyt c_3, and CNDS(i)|Lip^-·C_4V^{2+} driven by the pH gradient in the absence of the electron flow were measured. As shown in Figure 6, the amount of passively transported H^+ increased linearly with time at the early stages, but it gradually deviates downward from a straight line. The passive flux of H^+ across the membrane can be expressed by the equations derived by Goldman[42] and Hodgkin and Katz[43]:

$$J_{H^+}^{o\to i} = P_{H^+}\frac{FV}{RT}\frac{[H^+]_i - [H^+]_o \exp[-FV/(RT)]}{\exp[-FV/(RT)] - 1} \quad (9)$$

$$V = \frac{RT}{F}\ln\frac{P_{H^+}[H^+]_o + P_{OH^-}[OH^-]_i}{P_{H^+}[H^+]_i + P_{OH^-}[OH^-]_o} \quad (10)^{44}$$

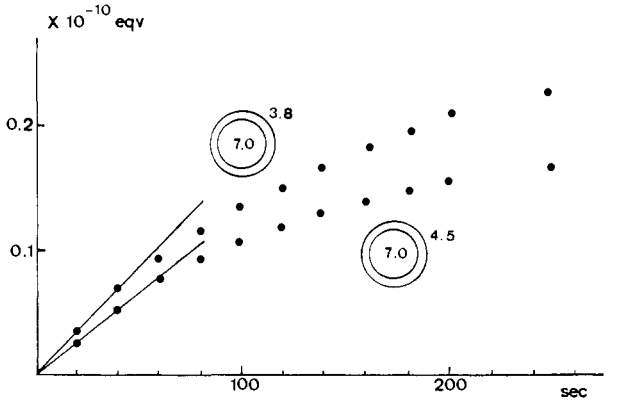

Figure 6. Passive transport of H^+ driven by pH gradient.

where J_{H^+} and P_{H^+} are the net flux of H^+ and permeability coefficient of membrane to H^+, respectively. The subscripts o and i refer to outside and inside, respectively, and V is the electrical potential across the membrane. J_{H^+} can be expressed by eq 11,

$$J_{H^+} = P_{H^+}([H^+]_o - [H^+]_i) \qquad (V \ll 1) \quad (11)$$

for small V values and by use of eq 11. Thus P_{H^+} was estimated to be 1.1×10^{-8} cm/s under the present conditions from the observed straight line shown in Figure 6.

Considering the difference between the permeabilities of sonicated and ether-injected liposomal membranes to cations or anions (see Table IV), the value estimated above for H^+ permeability in the sonicated liposome indicates that the nature of the membranes was not changed significantly by the incorporation of cyt c_3 or C_4V^{2+}. The observed values also clearly demonstrate that proton permeation is slightly accelerated by the incorporation of cyt c_3, probably along the surface of the protein.

Mechanism of pH Gradient Generation: Simplified Concept of Coupling. As already discussed in the previous sections, we can compare active H^+ transport with passive H^+ transport. Active transport is "coupled" to electron transport and passive transport is driven by the pH gradient that is generated by the coupled H^+ influx. Interestingly, the coupled H^+ influx was much faster than the passive H^+ transport (Figures 5 and 6), producing a large pH gradient. The pH gradient is determined by the balance between H^+ influx and H^+ efflux. Therefore, the change of the interior H^+ concentration is shown by eq 12, where $J_{H^+}^{o\to i}$ is the H^+ influx

$$\frac{d[H^+]_i}{dt} = J_{H^+}^{o\to i} - P_{H^+}[H^+]_i \quad (12)^{45}$$

$$\text{maximum } [H^+]_i = J_{H^+}^{o\to i}/P_{H^+} \quad (13)$$

associated with the electron flow from outside to inside the liposome. Then the maximum concentration of the interior H^+ is obtained by eq 13. It is evident that the large pH gradient observed is due to rapid H^+ influx [i.e., rapid electron flow across the cyt c_3 (or C_4V^{2+}) membrane] and small H^+ permeability across the sonication membrane. Since $J_{H^+}^{o\to i}$ decreased with time (Figure 5), a theoretical upper limit of the interior H^+ concentration can be given by eq 14. According to eq 14, the theoretical

$$\text{theoretical maximum of } [H^+]_i = (J_{H^+}^{o\to i})_{t=0}/P_{H^+} \quad (14)$$

upper limit of the pH gradient across the membrane is estimated to be 4.2 for the cyt c_3–liposome and 4.0 for the C_4^{2+}–liposome.

(41) Tabushi, I.; Nishiya, T.; Yagi, T.; Inokuchi, H. *Tetrahedron Lett.* **1981**, *22*, 4989–4992.
(42) Goldman, D. E. *J. Gen. Physiol.* **1943**, *27*, 37–60.
(43) Hodgkin, A. L.; Katz, B. *J. Physiol. (London)* **1949**, *108*, 37–77.
(44) The electrical potential should be estimated by including all of the permeant ions in the constant field equation. However, considering the concentrations and permeabilities to ions present in the system, $K_3Fe(CN)_6$, CNDS, and Tris, contributions of $K_3Fe(CN)_6$, CNDS, or Tris to the electrical potential are negligibly small. Therefore, the electrical potential across the membrane can be approximated by using concentrations of H^+ and OH^- alone.
(45) Under our experimental conditions, contributions of other ions except H^+ and OH^- to the overall electrical potential are negligibly small and V is approximated as unity at the early stages of the reaction where inside pH and outside pH were very close.
(46) Papahadjopoulos, D.; Nir, S.; OhKi, S. *Biochim. Biophys. Acta* **1971**, *266*, 561–583.
(47) Hauser, H.; Phillips, M. C.; Stubbs, M. *Nature (London)* **1972**, *239*, 342–344.

These are of reasonable magnitude compared with the observed maximum pH gradients, 4.0 and 3.8, for the cyt c_3 and C_4V^{2+} liposomes, respectively. This fact strongly supports the proposed mechanism for the generation of the pH gradient.

For elucidation of the detailed mechanism of the observed accelerated H^+ influx coupled to the rapid electron flow, further investigations are necessary. However, we just wish to point out the following in order to clarify the situation.

The observed $J_{H^+}^{o\rightarrow i}$ was dependent on the outside reductant concentration at the early stages of the electron transport under the present conditions. It was also mildly affected by the pH gradient initially applied. Therefore, $\bar{J}_{H^+}^{o\rightarrow i}$ may be expressed by eq 15 where S is surface area. According to our preliminary

$$\lim_{t\rightarrow 0} \bar{J}_{H^+}^{o\rightarrow i}(\text{total}) = (\lim_{t\rightarrow 0} \bar{J}_{H^+}^{o\rightarrow i})S = \bar{P}_{H^+}[e]_o S \quad (15)$$

experiments, the permeability coefficient for the coupled H^+ flow, P_{H^+}, was larger than P_{H^+} by a factor of 10^1-10^2. This enhanced H^+ permeability plays the key role of coupling in the generation of a large pH gradient. A tentative mechanism for coupling, then, is that H^+ flow is associated with electron flow in order to maintain electroneutrality and thus H^+ flow is accelerated remarkably by rapid electron flow.

Registry No. Cytochrome c_3, 9035-44-3; $K_3Fe(CN)_6$, 13746-66-2; cytochrome c, 9007-43-6; C_4V^{2+}, 47082-19-9; hydrogen ion, 12408-02-5; hydroxide, 14280-30-9.

Conformational Effects in the Hydrolyses of Benzo-Ring Diol Epoxides That Have Bay-Region Diol Groups[1]

J. M. Sayer,*† D. L. Whalen,‡ S. L. Friedman,‡ A. Paik,‡ H. Yagi,† K. P. Vyas,† and D. M. Jerina†

Contribution from the Laboratory of Bioorganic Chemistry, National Institute of Arthritis, Diabetes, and Digestive and Kidney Diseases, National Institutes of Health, Bethesda, Maryland 20205, and the Laboratory for Chemical Dynamics, Department of Chemistry, University of Maryland Baltimore County, Baltimore, Maryland 21228.
Received March 10, 1983

Abstract: Kinetics of the hydronium ion catalyzed (k_H) and pH-independent (k_o) hydrolyses of several benzo-ring diol epoxides, derived from polycyclic aromatic hydrocarbons, that possess bay-region trans diol groups have been investigated in 1:9 dioxane–water at 25 °C. These epoxides are 1,2,3,4-tetrahydrobenz[*a*]anthracene-1,2-diol 3,4-epoxide, 1,2,3,4-tetrahydrotriphenylene-1,2-diol 3,4-epoxide, and 9,10,11,12-tetrahydrobenzo[*e*]pyrene-9,10-diol 11,12-epoxide. Both possible diastereomers of the diol epoxides in which the two hydroxyl groups are trans to each other were investigated: isomer **1**, in which the benzylic hydroxyl group is cis to the epoxide oxygen, and isomer **2**, in which this hydroxyl group and the epoxide oxygen are trans. The corresponding tetrahydro epoxides that lack a diol group were also investigated. For comparison, isomers **1** and **2** of 1,2,3,4-tetrahydrobenz[*a*]anthracene-3,4-diol 1,2-epoxide, a bay-region epoxide with a non-bay-region trans diol group, and the corresponding benzanthracene tetrahydro epoxide were also studied. The most striking feature of the reactions of the diol epoxides that possess a bay-region diol group is a reversal of the relative reactivity of isomers **1** and **2** in the k_o reaction, when compared with diol epoxides whose diol group is not in a bay region. This reversal of reactivity, which causes k_o to be larger for isomer **2** than for isomer **1** when the diol is in a bay region, is explained by changes in conformational equilibria involving the cyclohexene ring due to steric crowding of the bay-region diol. Preference of this diol group for a pseudodiaxial conformation favors a conformation of isomer **2** in which the benzylic C–O bond of the epoxide is more or less aligned with the π orbitals of the aromatic system and strongly disfavors this aligned conformation of isomer **1**. Reaction via the k_o process is faster for the aligned than for the nonaligned conformer; thus for epoxides with bay-region diol groups, k_o for isomer **2** is faster than k_o for isomer **1**. The pH-independent reaction of isomer **2** of 1,2,3,4-tetrahydrobenz[*a*]anthracene-1,2-diol 3,4-epoxide via the aligned conformer gives, in addition to cis and trans tetraol products, substantial quantitites of a keto diol, whereas no keto diol was detected from the corresponding isomer **1**. This also represents a reversal of the pattern of product formation generally observed with diol epoxides that lack a bay region in the vicinity of the diol group. Rate constants for hydronium ion catalyzed hydrolysis (k_H) are much less sensitive to conformational factors than k_o. The distribution of cis and trans tetraol products from hydronium ion catalyzed hydrolysis of the 1,2,3,4-tetrahydrobenz[*a*]anthracene-1,2-diol 3,4-epoxides and the 1,2,3,4-tetrahydrotriphenylene-1,2-diol 3,4-epoxides can be explained by preferential pseudoaxial attack of water upon the benzylic cations formed from these epoxides. On the basis of these observations and previous findings with non-bay-region diol, bay-region epoxides, rules for predicting the effects of conformation on rates and products of diol epoxide hydrolyses are proposed.

Benzo-ring diol epoxides in which the epoxide group forms part of a bay region of the hydrocarbon have been shown to be the most important ultimate carcinogens formed metabolically from a number of carcinogenic polycyclic aromatic hydrocarbons.[2] For benzo-ring diol epoxides in which the hydroxyl groups are trans to each other, two diastereomers are possible: diastereomer **1**, in which the epoxide oxygen is cis to the benzylic hydroxyl group, and diastereomer **2**, in which the epoxide oxygen is trans to this hydroxyl group (cf. Figure 1). Two rapidly interconvertible conformations of each diol epoxide are possible. In the absence of unusual steric or electronic factors, isomer **1** ordinarily has a slight preference for the conformation in which the hydroxyl groups are pseudodiaxial whereas isomer **2** has a relatively strong preference for the conformation in which the hydroxyl groups are pseudodiequatorial.[3-5] In the conformation normally preferred

† National Institutes of Health.
‡ University of Maryland Baltimore County.

(1) Supported in part by Public Health Service Grants Nos. CA-17278 and CA-26086 from the National Cancer Institute (D.L.W.).

(2) For a recent review and leading references see: Nordqvist, M.; Thakker, D. R.; Yagi, H.; Lehr, R. E.; Wood, A. W.; Levin, W.; Conney, A. H.; Jerina, D. M. In "Molecular Basis of Environmental Toxicity"; Bhatnagar, R. S., Ed.; Ann Arbor Science Publishers: Ann Arbor, MI, 1980; pp 329-357.

(3) (a) Yagi, H.; Hernandez, O.; Jerina, D. M. *J. Am. Chem. Soc.* **1975**, *97*, 6881-6883. (b) Yagi, H.; Thakker, D. R. Hernandez, O.; Koreeda, M.; Jerina, D. M. *Ibid.* 1977, *99*, 1604-1611.

0002-7863/84/1506-0226$01.50/0 © 1984 American Chemical Society